

Viral vector-mediated upregulation of serine racemase expression in medial prefrontal cortex improves learning and synaptic function in middle age rats

Brittney Yegla¹, Asha Rani¹, Ashok Kumar¹

¹Department of Neuroscience, McKnight Brain Institute, University of Florida, Gainesville, FL 32611, USA

Correspondence to: Ashok Kumar; email: kash@ufl.edu

Keywords: aging, medial prefrontal cortex, serine racemase, D-serine, NMDA receptor, cognitive flexibility

Received: January 19, 2023

Accepted: April 3, 2023

Published: April 12, 2023

Copyright: © 2023 Yegla et al. This is an open access article distributed under the terms of the [Creative Commons Attribution License](https://creativecommons.org/licenses/by/3.0/) (CC BY 3.0), which permits unrestricted use, distribution, and reproduction in any medium, provided the original author and source are credited.

ABSTRACT

An age-associated decrease in N-methyl-D-aspartate receptor (NMDAR)-mediated synaptic function contributes to impaired synaptic plasticity and is associated with cognitive impairments. Levels of serine racemase (SR), an enzyme that synthesizes D-serine, an NMDAR co-agonist, decline with age. Thus, enhancing NMDAR function via increased SR expression in middle age, when subtle declines in cognition emerge, was predicted to enhance performance on a prefrontal cortex-mediated task sensitive to aging. Middle-aged (~12 mo) male Fischer-344 rats were injected bilaterally in the medial prefrontal cortex (mPFC) with viral vector (LV), SR (LV-SR) or control (LV-GFP). Rats were trained on the operant attentional set-shift task (AST) to examine cognitive flexibility and attentional function. LV-SR rats exhibited a faster rate of learning compared to controls during visual discrimination of the AST. Extradimensional set shifting and reversal were not impacted. Immunohistochemical analyses demonstrated that LV-SR significantly increased SR expression in the mPFC. Electrophysiological characterization of synaptic transmission in the mPFC slices obtained from LV-GFP and LV-SR animals indicated a significant increase in isolated NMDAR-mediated synaptic responses in LV-SR slices. Thus, results of the current study demonstrated that prefrontal SR upregulation in middle age rats can improve learning of task contingencies for visual discrimination and increase glutamatergic synaptic transmission, including NMDAR activity.

INTRODUCTION

The function of N-methyl-D-aspartate receptors (NMDARs) has a profound influence on synaptic plasticity, cognition, psychiatric diseases, and connectivity of neural networks [1, 2]. Hippocampal and prefrontal cortex-dependent synaptic plasticity and cognitive capacities decline with advancing age [3–12]. More specifically, age-related changes in NMDARs, including subunit expression, corresponding neurotransmission, and oxidation-reduction status, are associated with age-related cognitive deficits. Age-related declines in NMDAR subunit expression, such as prefrontal GluN1 mRNA [13] and GluN2B protein in

the frontal and hippocampal regions [14], impact pharmacokinetics of glutamatergic transmission [15–17]. Reductions in NMDAR-mediated transmission significantly contribute to these age-related synaptic and cognitive impairments [18–26]. Using GluN2B knockout mice, loss of GluN2B in cortical and CA1 pyramidal neurons impaired NMDAR-mediated neurotransmission, decreased spine density in the CA1 of the hippocampus, and resulted in cognitive deficits dependent upon hippocampal and prefrontal function [27]. These neural and cognitive impairments align with those observed in aging. Conversely, upregulation of the GluN2B subunit recovers synaptic plasticity and spatial memory in aged animals [28, 29]. In addition to

subunit expression changes with aging, NMDAR function is modulated by oxidation-reduction status, and a higher level of oxidative stress is associated with advancing age, as well as cognitive impairment [21, 30–32].

D-serine, which is the primary co-agonist required for full activation of synaptic NMDARs, also decreases with aging [33–39]. D-serine is critical to synaptic plasticity and cognitive capacities [33, 36, 40–42]. D-serine levels are dependent upon serine racemase (SR), which is the enzyme that converts L-serine to D-serine [43–45]; correspondingly, levels of SR decline during aging [36, 37]. Deletion of SR affects hippocampal networks by altering the excitatory/inhibitory balance [46]. When age-related reductions in D-serine are supplemented with exogenous D-serine, synaptic transmission recovers in aged rodents in a dose-dependent manner, normalizing to young levels [12, 34, 36, 42].

Thus, upregulation of SR expression, which increases D-serine levels, may have therapeutic potential by upregulating NMDAR function. The beneficial effects of elevating D-serine in aging have been examined in relation to synaptic and cognitive capacities in the hippocampus. However, the prefrontal cortex (PFC), which is a brain region sensitive to disruptions in aging, has not been extensively evaluated. The PFC is involved in complex behaviors including executive function, which encompasses cognitive flexibility, inhibition, attention, and working memory [47, 48]. Executive dysfunction for working memory and cognitive flexibility also arises in middle age [49–51] and subtle attentional deficits associated with NMDAR impairments have been noted in middle age [52]. However, it is unknown if these deficits are related to NMDAR function, or more specifically D-serine availability.

We hypothesized that augmenting SR expression within mPFC glutamatergic neurons would improve attention and cognitive flexibility in middle-aged rats and facilitate synaptic responses in the mPFC. Thus, for this study, SR expression was upregulated in pyramidal neurons of the mPFC through lenti-viral technology to enhance NMDAR function and evaluate its impact on cognitive flexibility and NMDAR-mediated synaptic transmission in middle-age rats. The results demonstrate that viral vector-mediated upregulation of SR in the mPFC of middle-aged rats resulted in efficient contingency acquisition during visual discrimination, potentially through enhanced attentional function. Further, electrophysiological recordings demonstrated that up-regulation of SR expression significantly augmented NMDAR-mediated synaptic responses recorded from the mPFC.

RESULTS

LV-SR infusion increased prefrontal SR expression

To verify accurate expression of the SR viral vector, colocalization of GFP-positive cells and CaMKII-positive cells was evaluated within the mPFC (Figure 1B, 1C). Colocalization of GFP+/CaMKII+ cells was 52.48% in LV-SR-injected rats ($N = 7$). There was limited colocalization of GFP+/CaMKII+ cells in the control LV-GFP-injected rats (5.85%; $N = 9$). Injection of LV-SR increased the total area of fluorescence, indicative of SR levels, in the mPFC compared to LV-GFP-injected rats ($F_{(1,14)} = 12.59$, $p < 0.01$; Figure 1D, 1E).

Up-regulation of SR expression accelerated visual discrimination learning

Rats treated with LV-SR ($N = 7$) required fewer trials to attain criterion during the visual discrimination task ($F_{(1,14)} = 8.23$, $p = 0.01$; Figure 2A), suggesting that increased expression of SR accelerated learning of the task contingencies. LV-SR rats did not significantly differ from LV-GFP-treated rats ($N = 9$) for trials to criterion (TTC) when making an extradimensional shift during the set-shifting phase ($F_{(1,14)} = 2.49$, $p = 0.14$; Figure 2B), or a reversal ($F_{(1,14)} = 0.25$, $p = 0.63$; Figure 2C). Increasing SR levels also did not affect the number or the type of errors (i.e., perseverative, regressive, and never reinforced) made during set shift or reversal ($p > 0.05$). In addition, omissions did not vary by injection type ($p > 0.05$).

SR upregulation augments basal synaptic transmission

The effect of upregulation of SR expression on glutamatergic excitatory synaptic transmission was evaluated by recording and analyzing total fEPSPs from the mPFC slices in a subset of animals injected with LV-SR or LV-GFP vector. An input-output curve was generated by plotting the slope of the total synaptic response from LV-SR ($n = 8/4$ slices/animals) and LV-GFP ($n = 8/4$ slices/animals) rats as a function of increasing stimulation intensity (Figure 3). A repeated-measures ANOVA indicated main effects of increasing stimulation intensity ($F_{(9,126)} = 23.43$, $p < 0.0001$). A significant treatment by stimulation intensity interaction was observed ($F_{(9,126)} = 3.04$, $p < 0.003$) in absence of any main effect of treatment (Figure 3). However, repeated measures on higher stimulation intensities (20–40 volts) indicated that the total synaptic responses were higher in slices obtained from LV-SR-injected animals compared with LV-GFP, and there was a tendency for treatment effect ($F_{(1,14)} = 3.28$, $p < 0.09$).

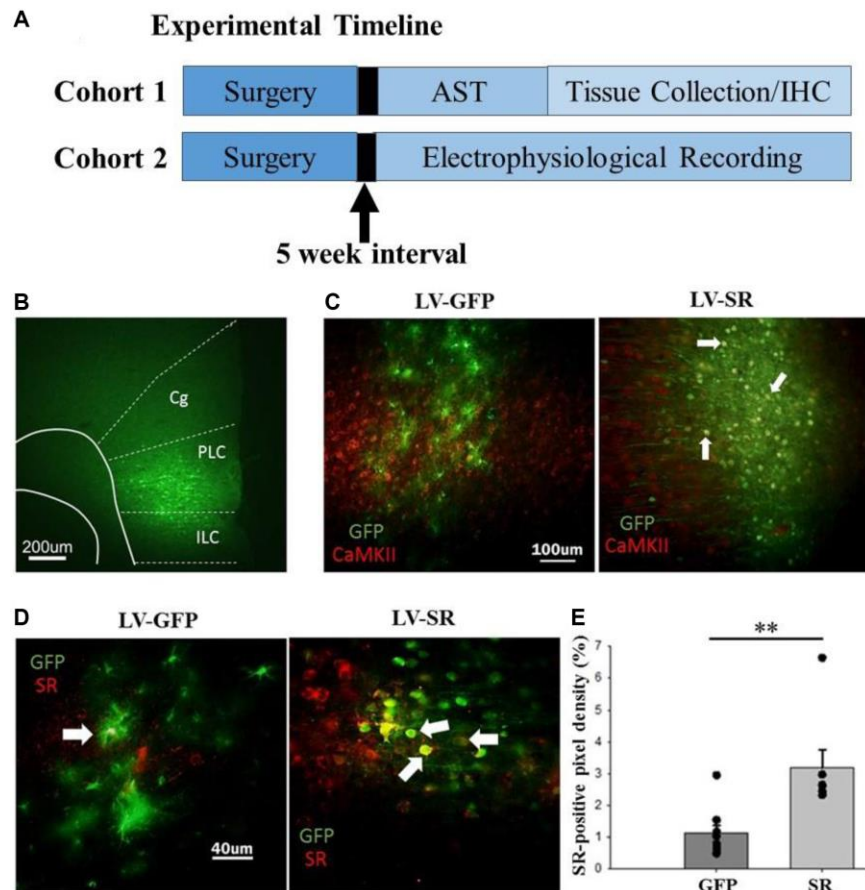


Figure 1. Experimental timeline and confirmation of lentiviral transfection and upregulation of SR expression in mPFC. (A) Experimental timeline illustrating details of experiments. Rats underwent surgery for lentiviral delivery into the mPFC and waited five weeks, to permit sufficient viral infection, before engaging in behavioral training on the attentional set shift task (AST) or electrophysiological recordings. Following AST, all rats were euthanized, had their tissue collected, and processed for immunohistochemistry (IHC). (B) Viral infection, represented as GFP+ expression, targeted the mPFC, which includes the cingulate (Cg), prelimbic (PLC), and infralimbic (ILC) cortices. (C) For rats injected with LV-SR ($N = 7$), viral infection (green, GFP) significantly overlapped with CaMKII+ cells (red; 52%). In contrast, rats injected with LV-GFP ($N = 9$), displayed limited overlap of GFP- (green) and CaMKII-positive cells (red). (D) Additional slices were evaluated for SR expression (red), and (E) based on further quantification (average of 4–7 slices/rat; individual rat's average represented as single data point) showed that LV-SR significantly increased SR levels in the mPFC where the virus (GFP represented in green) was expressed. Data represented as mean \pm SEM. ** $p < 0.01$.

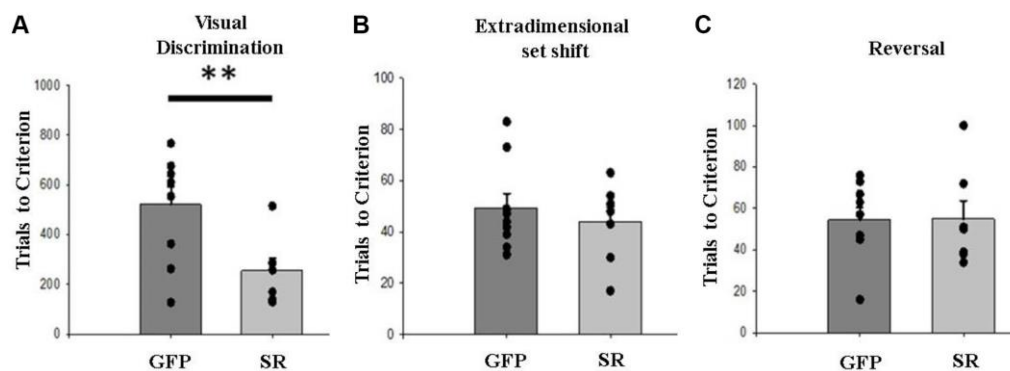


Figure 2. Upregulation of SR expression in mPFC accelerated learning an initial rule. (A) Middle-aged rats with LV-SR ($N = 7$) required fewer trials to reach criterion on visual discrimination than LV-GFP rats ($N = 9$). In contrast, LV-SR and LV-GFP rats did not significantly differ from one another regarding trials to criterion (TTC) for the extradimensional set shift (B) or reversal (C). Filled circles in (A–C) representing individual data points. Data represented as mean \pm SEM, with individual rat's performance displayed as single data point. ** $p < 0.01$.

The NMDAR-mediated synaptic component was pharmacologically isolated following the assessment of the total synaptic response. Input-output curves were constructed, and the synaptic response at each intensity was averaged across slices from the same animal (LV-SR: $n = 8/4$ slices/animals; LV-GFP: $n = 8/4$ slices/animals). An increase in the NMDAR-mediated synaptic response was observed for input-output curves plotting the NMDAR-fEPSPs slope as a factor of increasing stimulation intensity (Figure 4). A repeated-measures ANOVA indicated a significant main effect of stimulus intensity ($F_{(9,126)} = 34.59, p < 0.0001$) and treatment ($F_{(1,14)} = 9.41, p < 0.0001$) and an interaction of stimulation intensity and treatment ($F_{(9,126)} = 10.32, p < 0.0001$) on the slope of the recorded NMDAR-mediated synaptic

responses. *Post hoc* analyses indicated that the NMDAR synaptic responses were significantly ($p < 0.008$) augmented in slices from LV-SR-injected animals when compared with LV-GFP (Figure 4).

Redox regulation of NMDAR function

Based on previous findings using middle-aged rats, redox state was identified as a potential modulator of NMDAR synaptic responses [21]. To determine whether the increased expression of SR interacted with redox state to alter the NMDAR synaptic response, NMDAR responses in the mPFC were isolated and the reducing agent DTT (0.5 mM) was applied to slices obtained from LV-SR and LV-GFP rats (Figure 5A).

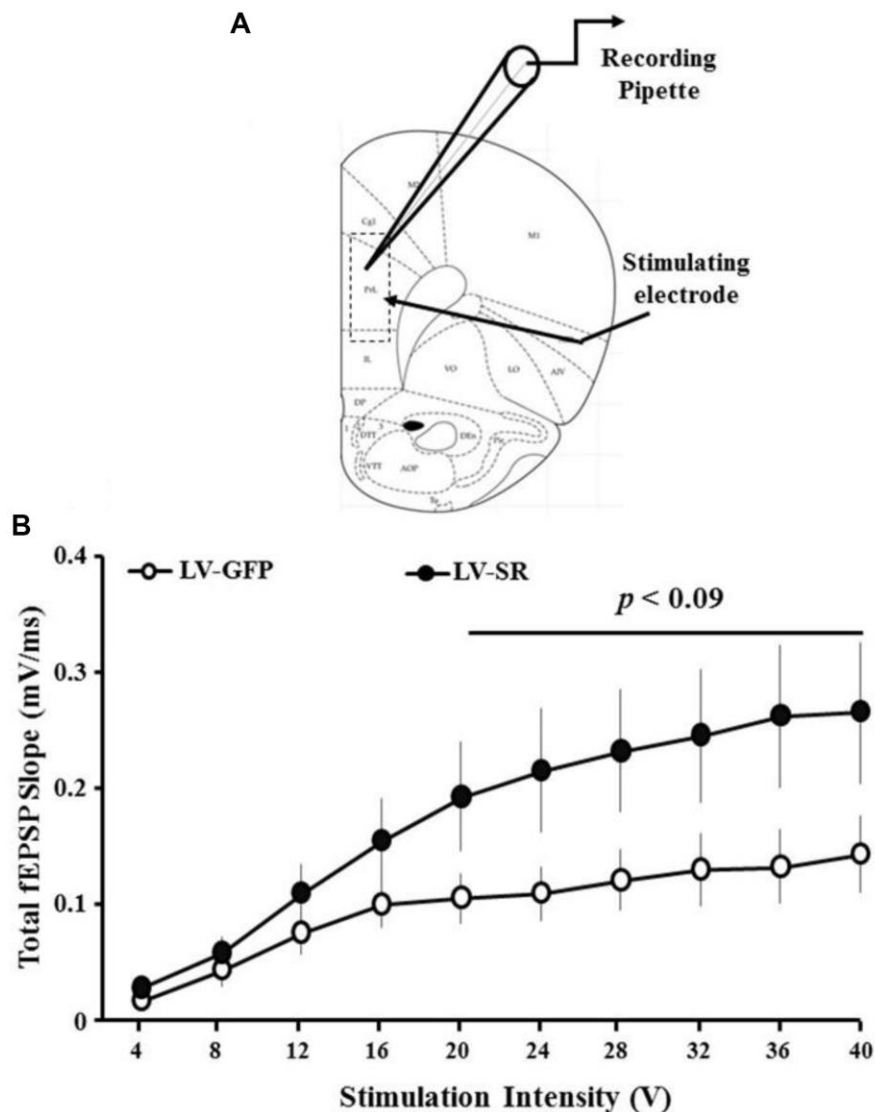


Figure 3. Upregulation of SR increased total synaptic strength. (A) Schematic of PFC slice adapted from Paxinos [108] illustrating location of recording and position of stimulating and recording electrodes. The rectangular dash lined box indicates the area used for recording total and NMDAR-mediated synaptic responses. (B) Input-output curve of total-fEPSP in slices obtained from LV-SR ($n = 8/4$ slices/animals) and LV-GFP ($n = 8/4$ slices/animals) animals, plotting the mean SEM slope across animals relative to increasing stimulation intensities. $p < 0.09$ represents a tendency for treatment effect at higher stimulation intensities (20–40V).

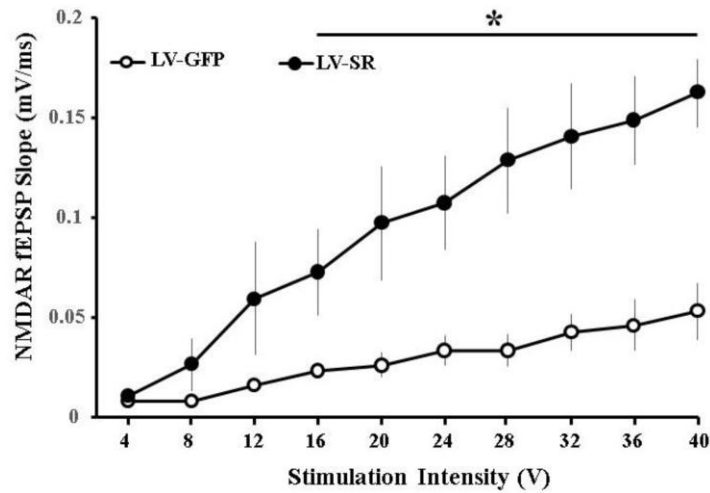


Figure 4. Upregulation of SR increased NMDAR-mediated synaptic response. Input-output curve of NMDAR-fEPSP in slices obtained from LV-SR ($n = 8/4$ slices/animals) and LV-GFP ($n = 8/4$ slices/animals) rats, plotting the mean SEM slope across animals relative to increasing stimulation intensities. *indicates a significant treatment difference at higher stimulation intensities (16–40V).

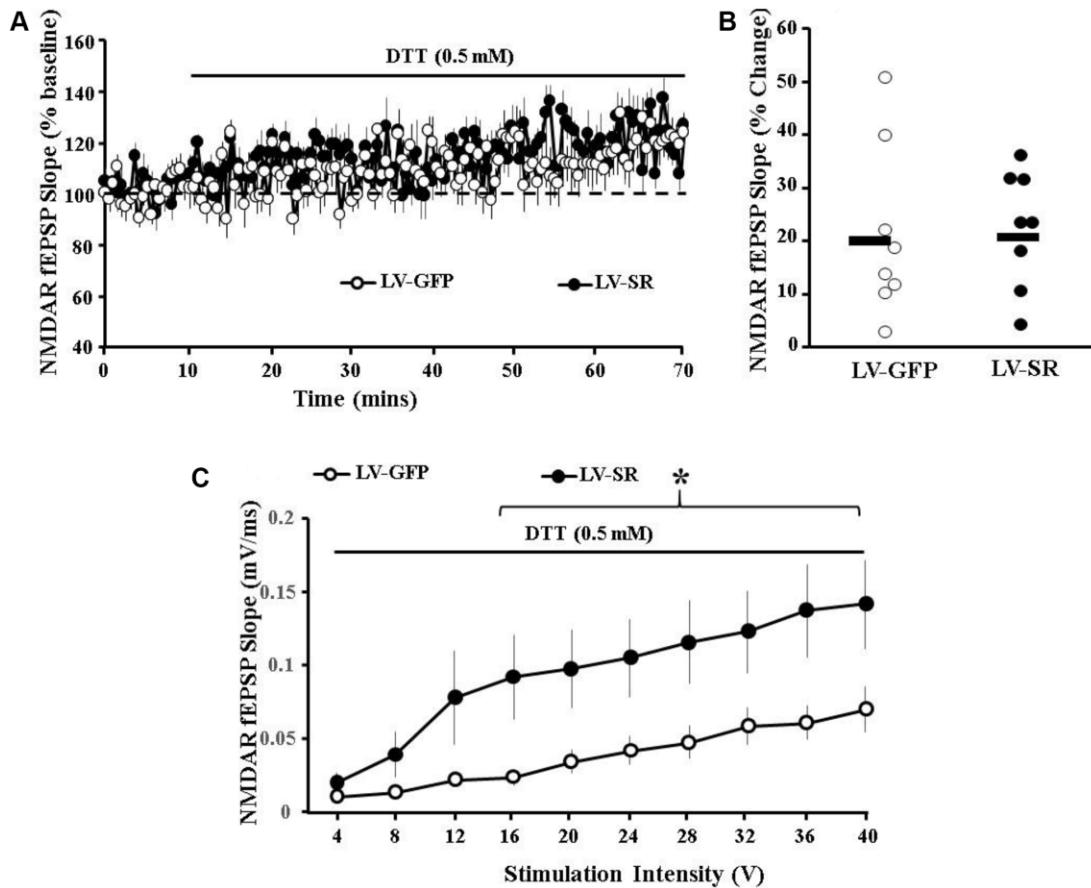


Figure 5. Redox regulation does not contribute to increased NMDAR synaptic function induced by upregulation of SR expression. (A) Time course of changes in the slope of the NMDAR-fEPSP obtained from mPFC slices 10 min before and up to 60 min after bath application of the reducing agent, DTT (0.5 mM; solid line) for slices obtained from LV-SR (filled circle, $n = 8/4$ slices/animals) and LV-GFP (control, open circle, $n = 8/4$ slices/animals) animals. (B) Scatter gram illustrating individual DTT-induced potentiation along with mean percentage increase (black solid line) in the slope of NMDAR-fEPSP in slices obtained from LV-SR (filled circle) and LV-GFP (open circle) animals. (C) Input-output curve of NMDAR-fEPSP slope in slices obtained from LV-GFP (open circle) and LV-SR (filled circle) rats 60 min following bath application of DTT (0.5 mM, solid line), across increasing stimulation intensities. *indicates a significant treatment difference at higher stimulation intensities (16–40V).

For LV-SR ($n = 8/4$ slices/animals) and LV-GFP ($n = 8/4$ slices/animals) animals, the NMDAR-fEPSP amplitude was maintained at $\sim 50\%$ of maximum, and a stable baseline was recorded for at least 10 min. Subsequent application of DTT resulted in a significant increase in the synaptic response from the baseline for both LV-SR ($p < 0.0007$) and LV-GFP ($p < 0.007$) animals (Figure 5B). However, the bath application of DTT did not increase the NMDAR-fEPSP differentially from LV-SR rats ($122.52 \pm 3.89\%$) compared with LV-GFP animals ($121.29 \pm 5.76\%$), indicating involvement of non-redox regulation to account for the enhanced NMDAR synaptic function in the mPFC observed following upregulation of SR (Figure 5C).

DISCUSSION

The results for the current study demonstrate that viral vector-mediated upregulation of SR, and putatively elevated D-serine levels in the mPFC, increased basal synaptic transmission in the PFC and improved acquisition of task contingencies for the visual discrimination condition. The lentiviral vector for SR, which was encoded with a CaMKII promoter, effectively infected glutamatergic pyramidal neurons in the PFC and increased SR expression at this site. Rats injected with LV-SR vector exhibited enhanced basal NMDAR-mediated synaptic transmission. These data suggest that the posited increase in D-serine from the elevated SR expression boosted NMDAR function in the mPFC of middle-aged rats.

In corroboration with these findings, D-serine has been identified as a critical co-agonist of NMDARs and is dependent on expression of SR, which converts L-serine to D-serine [43–45]. In the current study LV-SR, which colocalized with CaMKII-positive cells in the PFC, significantly increased SR expression and putatively increased D-serine levels. Surprisingly, LV-GFP did not exhibit strong colocalization with CaMKII-positive cells, despite also containing a CaMKII promoter, suggesting that the promoter was not selective in this specific viral vector, and is one weakness of this experiment. Both SR expression in neurons and L-serine shuttling in astrocytes are found to influence D-serine levels and alter CA1 synaptic neurotransmission [53]. D-serine may also be acting as an autocrine-signaling molecule, due to SR localization to postsynaptic regions of the neuron, including hippocampal pyramidal neurons and striatal GABAergic interneurons [54–57]. Moreover, despite the intention to target pyramidal neurons in the mPFC using the CaMKII promoter [58–60], this marker's expression has recently been observed in parvalbumin or somatostatin interneurons from the superficial motor cortex of mice [61]. Thus, other neuronal types may have been

transfected by LV-GFP or LV-SR and influenced SR expression. Thus, other neuronal types may have been transfected by LV-GFP or LV-SR and influenced SR expression. Notably, the LV-SR group exhibited significantly higher SR expression than the LV-GFP group, demonstrating that the LV-SR vector was efficacious.

In agreement with the hippocampal literature demonstrating the enhancing effects of D-serine on NMDAR-related function, the LV-SR group displayed increased basal NMDAR-mediated transmission in the mPFC. Previous studies have shown that application of D-serine enhanced evoked NMDAR-mediated currents in both hippocampal CA1 pyramidal neurons and interneurons, though to differing degrees potentially due to NMDAR subunit composition [62]. Endogenous sources of astrocytic D-serine also significantly contributed to NMDAR activity and long-term potentiation (LTP) [63]. Conversely, in SR knockout mice Ploux and colleagues (2020), amongst others [46, 64, 65], observed a weakening of NMDAR responses and LTP. Interestingly, this NMDAR hypofunction was observed in SR knockouts despite a natural compensatory mechanism of increased hippocampal expression of glycine, which also binds at the co-agonist site on the NMDAR.

Impaired NMDAR- and non-NMDAR-mediated glutamatergic transmission in the hippocampus during normal aging is strongly related to cognitive dysfunction, such as executive function and memory [66–68]. Engagement of the D-serine pathway has shown significant benefits in hippocampal-dependent NMDAR-mediated transmission and cognitive function in preclinical models of aging. In the aging brain, D-serine levels and NMDAR-mediated synaptic transmission are reduced [33–39], whereas supplementation with exogenous D-serine in aged rats [34] or mice with low D-serine release due to astrocytic mutations [69] normalize hypofunctional NMDAR responses. Moreover, the beneficial effects of sAPP α , a secreted form of amyloid precursor protein generated by the non-amyloidogenic pathway, on NMDAR-mediated transmission in hippocampal slices of aged mice are partially mediated by the D-serine pathway, as evidenced by an attenuation of these enhancing effects in SR knockout mice [70]. These beneficial effects of D-serine have translated to amelioration of cognitive function in elderly as well. Healthy older adults receiving D-serine supplementation exhibited improved spatial memory, learning, and problem solving, with greater effects observed for those with higher plasma D-serine levels [71]. Thus, D-serine bolsters glutamatergic transmission and cognitive function and could potentially attenuate age-related cognitive decline [72].

Initial cognitive impairments arising in aging include those dependent upon executive function, such as attention. To evaluate if increased expression of SR could improve one such cognitive capacity (i.e., cognitive flexibility) in middle-aged rats, we measured visual discrimination, attentional set shifting, and reversal learning. Set shifting is primarily dependent upon the mPFC [73, 74] while reversal learning relies upon the orbitofrontal cortex (OFC) [75–77]. In addition, dynamic interactions between the OFC and hippocampus for reversal learning have been noted, with local field potentials of the OFC and hippocampus exhibiting coherence in theta rhythm in a performance-dependent manner [78, 79] and contralateral lesions of the OFC and ventral hippocampus in mice subtly, though significantly, impairing spatial reversal learning [78]. Systemic D-serine treatment has shown beneficial effects on spatial reversal learning [69, 80–83]. However, for this study, upregulation of SR in the mPFC did not affect reversal. Given that the lentiviral injection targeted the mPFC rather than the OFC, the lack of effects on reversal learning observed in this study aligns with the literature regarding the critical role of the OFC and hippocampus, rather than the mPFC, to this cognitive capacity.

By targeting the mPFC with LV-SR, enhancement in set-shifting performance would have been expected. However, no effects of manipulation were noted on this measure. Few studies have evaluated the impact of D-serine in set-shifting, but there is evidence of glutamatergic signaling impacting set-shifting and reversal learning performance. In adult rodents, disruption of medial prefrontal NMDAR or AMPA receptor function impaired set-shift performance, increasing perseverative errors, but had no effect on reversal learning [84–86]. More selective manipulations, targeting GluN2A and GluN2B specifically, have demonstrated their important role in extradimensional set-shifting and spatial reversal learning [80, 87–89]. In terms of aging, age-related reductions in GluN1 expression in the mPFC were correlated with impaired set-shifting performance in aged rats, while expression of AMPA receptor subunits that were found to be decreased with aging (GluR1, GluR2) did not relate to set-shifting performance [90]. Therefore, enhanced NMDAR-mediated function via purported increases in D-serine would be expected to improve set-shifting. Despite increased NMDAR-mediated transmission in the mPFC in this study, corresponding changes in set-shifting did not emerge. This may be due to lower levels of D-serine attained in this study (through the elevation of SR expression) than was observed or used in other studies. The exact levels of D-serine in the mPFC were not measured and is a limitation of this study.

LV-SR infusion in the mPFC accelerated learning in the visual discrimination condition, as noted by the reduced trials to criterion. In agreement with these findings, NMDAR hypofunction impairs visual discrimination, as observed with NMDAR antagonists [91–93], deletion of the GluN1 subunit on dopaminergic neurons [94], and GluN2A knockouts [95, 96]. This is the first study to demonstrate that enhanced basal NMDAR synaptic function, via viral vector-mediated upregulation of SR expression in mPFC of middle-aged rats, was associated with improved visual discrimination learning. The results from this study support the beneficial effects of the D-serine pathway involvement in NMDAR-mediated transmission and cognitive function, expanding the literature to emphasize its role in not only the hippocampus but also the PFC. Thus, targeting this pathway could pose a potential route in reversing age-related cognitive decline and should be considered for future research.

MATERIALS AND METHODS

Subjects

Middle-age male Fischer-344 rats (~12-month) were obtained from the National Institute on Aging (Bethesda, MD, USA) and housed at the University of Florida in a temperature- and humidity-controlled vivarium on a 12:12 light/dark cycle (lights on: 7am). Rats remained pair-housed with full access to food and water and habituated to the facilities for a week prior to handling. Once acclimated and handled, rats underwent surgery for injection of either green fluorescent protein (GFP) or SR lentiviral vector with a Ca²⁺/calmodulin-dependent protein kinase II (CaMKII) promoter into the mPFC. After recovering for five weeks, rats were food restricted to 85% of their original weight, trained and tested on the attentional set-shift task (AST), following which they were perfused and brains were collected and examined for verification of viral expression. All procedures involving animals were approved by the Institutional Animal Care and Use Committee at the University of Florida and were in agreement with guidelines recognized by the U.S. Public Health Service Policy on Humane Care and Use of Laboratory Animals. A schematic of experiment timeline is provided in Figure 1A.

Lentiviral vector and mPFC injections

Lentiviral particles encoding SR (LV-SR) and green fluorescent protein (LV-GFP) were obtained from BioSource SAS-Genetic Engineering Technologies (GEG Tech, Paris, France). SR and GFP cDNAs were cloned into vectors containing a neuron specific promoter, CaMKII. Plasmids were packaged into

vesicular stomatitis virus (VSV) glycoprotein envelope before stereotaxic injections into the mPFC of male middle-aged rats. Rats were anesthetized with isoflurane in the induction chamber, and stereotaxic techniques (KOPE Stereotaxic Alignment System) were employed for virus injection. Lentiviral vector encoding SR (LV-SR, $\sim 1.0 \times 10^9$ transducing units/mL) or GFP (LV-GFP) was bilaterally injected into the mPFC (anterior/posterior +3.0 mm and medial/lateral ± 0.5 to 0.8 mm of bregma, dorsal/ventral 2.2 to 2.6 mm) using a glass pipette. Vector was injected bilaterally into mPFC and each injection consisted of $\sim 2 \mu\text{l}$ of SR or GFP vector. One cohort of rats was utilized for the behavior and immunohistochemical analyses, while a separate cohort of rats was used for the electrophysiology.

Attentional set shift task

Apparatus

The attentional set-shift task (AST) was conducted in rat operant boxes (Coulbourn Instruments, Whitehall, PA, USA), containing a food magazine port between two levers, which were located below two lights on the front panel. A house light was positioned on the rear wall. Operant boxes were individually stored within a sound-attenuating chamber with a fan for aeration and noise dampening. The input and output from each box were transmitted to Graphic State 4 software (Coulbourn Instruments) on an Optiplex 9020 computer.

Behavioral paradigm

Once rats fully recovered from surgery (\sim five weeks), they were food restricted to 85% of their starting body weight. Rats were exposed to the food reward pellets in their home cage during this period to reduce neophobia. The task was modified from Floresco et al., 2008 [74, 97, 98]. For two days, rats were habituated to the operant chamber for 15 min, with the back house light on and 10 food pellets in the magazine. Rats were trained to lever press, whereby they had 30 min to hit the extended levers on an FR-1 schedule for a food pellet reward. Once they pressed each lever 50 times, rats transitioned to sessions in which the levers were extended for 10 s for each trial. If no response was made, a “time out” period of 10 s occurred where the house light extinguished, and an omission was recorded. During the lever presentation, one of the two front panel lights was pseudo-randomly illuminated to expose the rats to this stimulus. Rats needed 90% performance before being evaluated for a side bias. During the side bias assessment, rats performed seven trials and had to alternate between each lever. Whichever lever they displayed a persistent preference for was not selected as their “Set shift” lever (see below). Rats progressed to a visual discrimination (VD) paradigm, in which the

location of the light cue predicted the rewarded lever (the lever below the light). For criterion of VD and later stages (the extra-dimensional shift and reversal), rats needed to correctly perform 8 consecutive trials and greater than 30 trials total to progress to the next stage. Each session consisted of 120 trials maximum, and rats continued with the same phase until they reached criterion. The time out period remained at 10s and the inter-trial interval was 9–12s. After VD, rats made an extradimensional shift (set-shift) from the light cue as the predictor to an egocentric response, whereby the location of the lever itself (right or left of the rat) predicted the reward. Once rats attained criterion on the set-shift paradigm, the rewarding response was reversed (i.e., a reversal) to the opposite lever location.

Behavioral analysis

The number of trials to criterion served as a measure of the rats’ capacity to learn a new strategy, as well as make an extra-dimensional set shift and reversal. Total omissions, calculated as (trials omitted/total trials) \times 100, were also measured. Performance errors were recorded and, during the set-shift paradigm, were characterized as perseverative, regressive, or never reinforced. Perseverative errors were defined as incorrect lever selection (i.e., below a light cue and thus perseverating to the VD strategy) when more than 70% of these errors were made. When fewer than 70% of these errors were made, the incorrect selections were defined as regressive errors, indicative of a gradual shift to the new response strategy. During VD and reversal stages, only total errors were calculated.

Immunohistochemistry

Tissue collection

Rats were anesthetized with isoflurane and underwent transcardial perfusion with 200 mL of ice cold 1X phosphate buffered saline (PBS) and 4% paraformaldehyde (PFA). Brains were extracted, placed in 4% PFA for overnight incubation at 4°C, and transferred to 30% sucrose. After sinking in the solution, brains were embedded in OCT and maintained at -80°C until slicing. Brains were sliced on a cryostat (Microm, Waltham, MA, USA), as 40 μm -thick coronal sections, and the prefrontal cortical region was collected and maintained in cryoprotectant solution (30% ethylene glycol, 15% glucose, 0.04% sodium azide in 0.05M PBS).

Immunofluorescent procedure

Six sections of the PFC (A/P range: +4 to +2) were processed for co-localization of CaMKII, which was the promoter of both lentiviruses, and GFP, which served as an indicator of the viral vector infusion site for LV-GFP and LV-SR groups. As previously conducted [99]

coronal sections were rinsed thrice for 5 min in 1X tris-buffered saline (TBS), incubated in antigen retrieval solution (Vector, Burlingame, CA, USA) for 10 min at 95°C, rinsed again, and blocked in 10% donkey serum for 1 hr. Sections were then incubated at 4°C for 48 hrs for mouse anti-CaMKII (1:1000, Invitrogen, Carlsbad, CA, USA) and 24 hrs for rabbit anti-GFP (1:500; Invitrogen) in 1% donkey serum. Slices were then rinsed in TBS and 1% Triton X100 and incubated in 1% donkey serum with AlexaFluor-488 donkey anti-mouse (1:500; Invitrogen) and donkey anti-rabbit-594 (1:500; Jackson, Westgrove, PA, USA). Slices were rinsed 3 × 5 min in TBS, mounted onto slides and cover slipped with DAPI (Vector).

An additional set of prefrontal slices underwent free-floating immunohistochemistry for SR expression, to confirm the efficacy of the LV-SR in increasing SR levels in the PFC. Slices were rinsed thrice for 5 min in 1X PBS, heated at 95°C for 10 min in antigen retrieval solution (Vector), rinsed, and blocked for 2 hrs in 10% donkey serum and 0.3% Triton in 1X PBS. Sections were incubated overnight at 4°C in 1% bovine serum albumin (BSA) in PBS with mouse anti-serine racemase (1:100, Santa Cruz, Dallas, TX, USA). Free-floating sections were rinsed thrice and incubated for 2 hrs in secondary antibody (donkey anti-mouse-488; 1:500; Invitrogen) in 1% BSA. Sections were rinsed, mounted onto slides and cover slipped with mounting media containing DAPI (Vector).

Image analysis

Slices fluorescently tagged for co-localization of GFP/CaMKII were imaged at 200× magnification, while SR-tagged slices were imaged at 400×, on a Leica DM2500 microscope (Wetzlar, Germany), equipped with a Retiga 4000R camera (QImaging, Surrey, BC, Canada) and QCapture Pro7 software (QImaging). Images were then enhanced for improved visualization using Adobe Photoshop (San Jose, CA, USA) prior to co-localization analysis, which was calculated as [(CaMKII+ and GFP+)/all GFP+] × 100. Approximately 100 GFP-positive cells at the infusion site were included for each animal. To evaluate SR expression, images were converted from pixels to micrometer (56pixels/μm) and enhanced to reduce background noise, and the total area with positive fluorescent tagging in the mPFC was calculated using NIH *ImageJ*. Tissue from LV-GFP (*N* = 9) and LV-SR (*N* = 7) were then analyzed for statistical differences in SR expression.

Electrophysiology

mPFC slice preparation

The protocol for preparation of mPFC slices for electrophysiological studies were modified from

standardized lab protocols [20–23, 30, 99–105]. Animals were deeply anesthetized using isoflurane and decapitated with a guillotine (MyNeuroLab, St Louis, MO, USA). The brain was rapidly removed and transferred into a beaker containing ice-cold artificial cerebrospinal fluid (aCSF). The PFC was blocked and coronal slices (~400 μm) were cut using a tissue chopper (Mickle Laboratory Engineering Co, Surrey, UK). The freshly cut slices were incubated in a holding chamber (at room temperature) with aCSF containing (in mM): 124 NaCl, 2 KCl, 1.25 KH₂PO₄, 2 MgSO₄, 2 CaCl₂, 26 NaHCO₃, and 10 D-glucose. Slices were transferred to a standard interface recording chamber (Warner Instrument, Hamden, CT, USA) at least thirty minutes before recording. The chamber was continuously perfused with oxygenated aCSF (95%-O₂ and 5%-CO₂) at the rate of 2 mL/min and the temperature was maintained at approximately 37°C using the TC-324B temperature controller (Warner Instrument, Hamden, CT, USA). The pH of the aCSF was maintained at 7.4.

Extracellular field potential recordings

Extracellular field excitatory postsynaptic potentials (fEPSPs) were recorded using a glass micropipette electrode filled with aCSF. The glass micropipettes were pulled from thin-walled borosilicate capillary glass using a Flaming Brown horizontal micropipette puller (Sutter Instruments, San Rafael, CA, USA), and the electrode resistances ranged from 4–6 MΩ. The recording pipette was localized to layer 2/3 of the mPFC (Figure 4). A concentric bipolar stimulating electrode (FHC, Bowdoinham, ME, USA) was localized to layer 4/5. Diphasic stimulus pulses (100 μsec, SD9 Stimulator, Grass Instrument Co., West Warwick, RI, USA) were delivered to layer 4/5 of the mPFC (0.033 Hz) to evoke fEPSPs. The signals were sampled at a frequency of 20-kHz, amplified and filtered between 1 Hz and 1 kHz using Axoclamp-2A (Molecular Devices, Sunnyvale, CA, USA) and a differential AC amplifier (A-M Systems, Sequim, WA, USA). Field potential data were stored on a computer hard drive (Dell Inc., TX, USA) for off-line analysis. A separate output from the differential AC amplifier was fed into an oscilloscope (Tektronix 2214, Tektronix Inc., Beaverton, OR, USA) for real time visualization of the signals. In order to measure the amplitude of the fEPSP, two cursors were placed to encompass the entire waveform. A Sciworks computer algorithm (Datawave Technologies, Berthoud, CO, USA) was used to compute the maximum amplitude (mV) of the fEPSP at the peak of the waveform, as well as the slope of the descending response. In order to measure the slope of the fEPSP, two cursors were placed around the initial descending phase of the waveform and the maximum slope (mV/ms) of the fEPSP was determined by a

computer algorithm that found the maximum change across all sets of 20 consecutively recorded points between the two cursors. Input-output curves for the slope of the total fEPSP were constructed for increasing stimulation intensities.

Isolation of NMDAR-mediated synaptic response

Following collection of the total synaptic response, the NMDAR-mediated field excitatory postsynaptic potentials (NMDAR-fEPSPs) were isolated and recorded as described previously [20, 30, 99, 100, 104, 105]. In order to obtain the NMDAR-fEPSP, mPFC slices were incubated in aCSF containing a low concentration of extracellular Mg²⁺ (0.5 mM), 6,7-dinitroquinoxaline-2,3-dione (DNQX, 30 μM), and picrotoxin (10 μM). Input-output curves for the NMDAR-fEPSPs were constructed for increasing stimulation intensities. In some cases, pharmacological isolation of the NMDAR-fEPSPs was confirmed by the application of the NMDAR antagonist AP-5 (100 μM).

Our previous results demonstrate that redox state modulates NMDAR-mediated synaptic function in mPFC [20], so we investigated whether the increased expression of SR interacted with redox state to alter the NMDAR synaptic response. To examine the effects of the reducing agent, dithiothreitol (DTT), the baseline response was set at ~50% of the maximum, and responses were collected for at least 10 min before and 60–70 min after drug application. The DTT dose (0.5 mM) was selected due to previous studies that showed that this dose was within a range that can increase NMDAR responses in aged animals and in young animals under oxidizing conditions, yet is below a dose that impairs enzyme activity [21, 30, 106, 107].

Statistical analysis

Examining the impact of LV-SR infusion into the mPFC, a one-way analysis of variance (ANOVA) was applied to the immunohistochemical and behavioral data, with infusion type as the between-subjects factor. Under conditions where homoscedasticity or normality were violated, the Brown-Forsythe or Mann-Whitney U statistic was applied, respectively. For electrophysiological recordings, repeated-measures ANOVAs, with stimulation as the repeated measure, were conducted. Significant differences were localized using Fischer's PLSD *post hoc* comparisons ($p < 0.05$), and data were interpreted as significant if $p \leq 0.05$.

AUTHOR CONTRIBUTIONS

BY, performed experiments, analyzed data, constructed illustrations, and wrote manuscript, AR performed experiments; AK designed and performed experiments,

analyzed data, constructed illustrations, and wrote the manuscript.

CONFLICTS OF INTEREST

The authors declare no conflicts of interest related to this study. Brittney Yegla currently works at Supernus Pharmaceuticals, though the company did not sponsor or support this work.

ETHICAL STATEMENT

All procedures involving animals were approved by the Institutional Animal Care and Use Committee at the University of Florida and were in agreement with guidelines recognized by the U.S. Public Health Service Policy on Humane Care and Use of Laboratory Animals.

FUNDING

This work was supported by National Institute of Aging grants R21AG068205 and R01AG037984, and the Evelyn F. McKnight Brain Research Foundation. Special thanks Dr. Thomas C Foster for his expert advice on introduction and discussion along with letting us use his lab resources. Thanks to Asharde Ward, Noelle Graghty, Olivia Boczniewicz, Ilex Wass de Czege, and Michael Lafferty, for their assistance in animal handling and surgery.

REFERENCES

1. Dore K, Stein IS, Brock JA, Castillo PE, Zito K, Sjöström PJ. Unconventional NMDA Receptor Signaling. *J Neurosci*. 2017; 37:10800–7. <https://doi.org/10.1523/JNEUROSCI.1825-17.2017> PMID:[29118208](https://pubmed.ncbi.nlm.nih.gov/29118208/)
2. Zorumski CF, Izumi Y. NMDA receptors and metaplasticity: mechanisms and possible roles in neuropsychiatric disorders. *Neurosci Biobehav Rev*. 2012; 36:989–1000. <https://doi.org/10.1016/j.neubiorev.2011.12.011> PMID:[22230702](https://pubmed.ncbi.nlm.nih.gov/22230702/)
3. Billard JM. Ageing, hippocampal synaptic activity and magnesium. *Magnes Res*. 2006; 19:199–215. PMID:[17172010](https://pubmed.ncbi.nlm.nih.gov/17172010/)
4. Lynch MA. Age-related impairment in long-term potentiation in hippocampus: a role for the cytokine, interleukin-1 beta? *Prog Neurobiol*. 1998; 56:571–89. [https://doi.org/10.1016/s0301-0082\(98\)00054-9](https://doi.org/10.1016/s0301-0082(98)00054-9) PMID:[9775404](https://pubmed.ncbi.nlm.nih.gov/9775404/)
5. Barnes CA. Long-term potentiation and the ageing brain. *Philos Trans R Soc Lond B Biol Sci*. 2003;

- 358:765–72.
<https://doi.org/10.1098/rstb.2002.1244>
PMID:[12740124](https://pubmed.ncbi.nlm.nih.gov/12740124/)
6. Foster TC. Involvement of hippocampal synaptic plasticity in age-related memory decline. *Brain Res Brain Res Rev.* 1999; 30:236–49.
[https://doi.org/10.1016/s0165-0173\(99\)00017-x](https://doi.org/10.1016/s0165-0173(99)00017-x)
PMID:[10567726](https://pubmed.ncbi.nlm.nih.gov/10567726/)
 7. Dumitriu D, Hao J, Hara Y, Kaufmann J, Janssen WG, Lou W, Rapp PR, Morrison JH. Selective changes in thin spine density and morphology in monkey prefrontal cortex correlate with aging-related cognitive impairment. *J Neurosci.* 2010; 30:7507–15.
<https://doi.org/10.1523/JNEUROSCI.6410-09.2010>
PMID:[20519525](https://pubmed.ncbi.nlm.nih.gov/20519525/)
 8. Ianov L, De Both M, Chawla MK, Rani A, Kennedy AJ, Piras I, Day JJ, Siniard A, Kumar A, Sweatt JD, Barnes CA, Huentelman MJ, Foster TC. Hippocampal Transcriptomic Profiles: Subfield Vulnerability to Age and Cognitive Impairment. *Front Aging Neurosci.* 2017; 9:383.
<https://doi.org/10.3389/fnagi.2017.00383>
PMID:[29276487](https://pubmed.ncbi.nlm.nih.gov/29276487/)
 9. Legon W, Punzell S, Dowlati E, Adams SE, Stiles AB, Moran RJ. Altered Prefrontal Excitation/Inhibition Balance and Prefrontal Output: Markers of Aging in Human Memory Networks. *Cereb Cortex.* 2016; 26:4315–26.
<https://doi.org/10.1093/cercor/bhv200>
PMID:[26400915](https://pubmed.ncbi.nlm.nih.gov/26400915/)
 10. Luebke JI, Chang YM, Moore TL, Rosene DL. Normal aging results in decreased synaptic excitation and increased synaptic inhibition of layer 2/3 pyramidal cells in the monkey prefrontal cortex. *Neuroscience.* 2004; 125:277–88.
<https://doi.org/10.1016/j.neuroscience.2004.01.035>
PMID:[15051166](https://pubmed.ncbi.nlm.nih.gov/15051166/)
 11. Morrison JH, Baxter MG. The ageing cortical synapse: hallmarks and implications for cognitive decline. *Nat Rev Neurosci.* 2012; 13:240–50.
<https://doi.org/10.1038/nrn3200>
PMID:[22395804](https://pubmed.ncbi.nlm.nih.gov/22395804/)
 12. Potier B, Turpin FR, Sinet PM, Rouaud E, Mothet JP, Videau C, Epelbaum J, Dutar P, Billard JM. Contribution of the d-Serine-Dependent Pathway to the Cellular Mechanisms Underlying Cognitive Aging. *Front Aging Neurosci.* 2010; 2:1.
<https://doi.org/10.3389/neuro.24.001.2010>
PMID:[20552041](https://pubmed.ncbi.nlm.nih.gov/20552041/)
 13. Magnusson KR, Bai L, Zhao X. The effects of aging on different C-terminal splice forms of the zeta1(NR1) subunit of the N-methyl-d-aspartate receptor in mice. *Brain Res Mol Brain Res.* 2005; 135:141–9.
<https://doi.org/10.1016/j.molbrainres.2004.12.012>
PMID:[15857677](https://pubmed.ncbi.nlm.nih.gov/15857677/)
 14. Zhao X, Rosenke R, Kronemann D, Brim B, Das SR, Dunah AW, Magnusson KR. The effects of aging on N-methyl-D-aspartate receptor subunits in the synaptic membrane and relationships to long-term spatial memory. *Neuroscience.* 2009; 162:933–45.
<https://doi.org/10.1016/j.neuroscience.2009.05.018>
PMID:[19446010](https://pubmed.ncbi.nlm.nih.gov/19446010/)
 15. Kim MJ, Dunah AW, Wang YT, Sheng M. Differential roles of NR2A- and NR2B-containing NMDA receptors in Ras-ERK signaling and AMPA receptor trafficking. *Neuron.* 2005; 46:745–60.
<https://doi.org/10.1016/j.neuron.2005.04.031>
PMID:[15924861](https://pubmed.ncbi.nlm.nih.gov/15924861/)
 16. Monaghan DT, Jane DE. Pharmacology of NMDA Receptors. In: Van Dongen AM, editor. *Biology of the NMDA Receptor.* Boca Raton (FL): CRC Press/Taylor & Francis; 2009.
PMID:[21204415](https://pubmed.ncbi.nlm.nih.gov/21204415/)
 17. Singh P, Doshi S, Spaethling JM, Hockenberry AJ, Patel TP, Geddes-Klein DM, Lynch DR, Meaney DF. N-methyl-D-aspartate receptor mechanosensitivity is governed by C terminus of NR2B subunit. *J Biol Chem.* 2012; 287:4348–59.
<https://doi.org/10.1074/jbc.M111.253740>
PMID:[22179603](https://pubmed.ncbi.nlm.nih.gov/22179603/)
 18. Barnes CA, Rao G, Shen J. Age-related decrease in the N-methyl-D-aspartateR-mediated excitatory postsynaptic potential in hippocampal region CA1. *Neurobiol Aging.* 1997; 18:445–52.
[https://doi.org/10.1016/s0197-4580\(97\)00044-4](https://doi.org/10.1016/s0197-4580(97)00044-4)
PMID:[9330977](https://pubmed.ncbi.nlm.nih.gov/9330977/)
 19. Foster TC. Dissecting the age-related decline on spatial learning and memory tasks in rodent models: N-methyl-D-aspartate receptors and voltage-dependent Ca²⁺ channels in senescent synaptic plasticity. *Prog Neurobiol.* 2012; 96:283–303.
<https://doi.org/10.1016/j.pneurobio.2012.01.007>
PMID:[22307057](https://pubmed.ncbi.nlm.nih.gov/22307057/)
 20. Guidi M, Kumar A, Foster TC. Impaired attention and synaptic senescence of the prefrontal cortex involves redox regulation of NMDA receptors. *J Neurosci.* 2015; 35:3966–77.
<https://doi.org/10.1523/JNEUROSCI.3523-14.2015>
PMID:[25740525](https://pubmed.ncbi.nlm.nih.gov/25740525/)
 21. Kumar A, Foster TC. Linking redox regulation of NMDAR synaptic function to cognitive decline during aging. *J Neurosci.* 2013; 33:15710–5.
<https://doi.org/10.1523/JNEUROSCI.2176-13.2013>
PMID:[24089479](https://pubmed.ncbi.nlm.nih.gov/24089479/)

22. Kumar A, Rani A, Scheinert RB, Ormerod BK, Foster TC. Nonsteroidal anti-inflammatory drug, indomethacin improves spatial memory and NMDA receptor function in aged animals. *Neurobiol Aging*. 2018; 70:184–93.
<https://doi.org/10.1016/j.neurobiolaging.2018.06.026>
PMID:[30031231](https://pubmed.ncbi.nlm.nih.gov/30031231/)
23. Kumar A, Thinschmidt JS, Foster TC. Subunit contribution to NMDA receptor hypofunction and redox sensitivity of hippocampal synaptic transmission during aging. *Aging (Albany NY)*. 2019; 11:5140–57.
<https://doi.org/10.18632/aging.102108>
PMID:[31339863](https://pubmed.ncbi.nlm.nih.gov/31339863/)
24. Magnusson KR, Scruggs B, Zhao X, Hammersmark R. Age-related declines in a two-day reference memory task are associated with changes in NMDA receptor subunits in mice. *BMC Neurosci*. 2007; 8:43.
<https://doi.org/10.1186/1471-2202-8-43>
PMID:[17587455](https://pubmed.ncbi.nlm.nih.gov/17587455/)
25. McQuail JA, Beas BS, Kelly KB, Simpson KL, Frazier CJ, Setlow B, Bizon JL. NR2A-Containing NMDARs in the Prefrontal Cortex Are Required for Working Memory and Associated with Age-Related Cognitive Decline. *J Neurosci*. 2016; 36:12537–48.
<https://doi.org/10.1523/JNEUROSCI.2332-16.2016>
PMID:[27807032](https://pubmed.ncbi.nlm.nih.gov/27807032/)
26. Potier B, Poindessous-Jazat F, Dutar P, Billard JM. NMDA receptor activation in the aged rat hippocampus. *Exp Gerontol*. 2000; 35:1185–99.
[https://doi.org/10.1016/s0531-5565\(00\)00122-4](https://doi.org/10.1016/s0531-5565(00)00122-4)
PMID:[11113601](https://pubmed.ncbi.nlm.nih.gov/11113601/)
27. Brigman JL, Wright T, Talani G, Prasad-Mulcare S, Jinde S, Seabold GK, Mathur P, Davis MI, Bock R, Gustin RM, Colbran RJ, Alvarez VA, Nakazawa K, et al. Loss of GluN2B-containing NMDA receptors in CA1 hippocampus and cortex impairs long-term depression, reduces dendritic spine density, and disrupts learning. *J Neurosci*. 2010; 30:4590–600.
<https://doi.org/10.1523/JNEUROSCI.0640-10.2010>
PMID:[20357110](https://pubmed.ncbi.nlm.nih.gov/20357110/)
28. Brim BL, Haskell R, Awedikian R, Ellinwood NM, Jin L, Kumar A, Foster TC, Magnusson KR. Memory in aged mice is rescued by enhanced expression of the GluN2B subunit of the NMDA receptor. *Behav Brain Res*. 2013; 238:211–26.
<https://doi.org/10.1016/j.bbr.2012.10.026>
PMID:[23103326](https://pubmed.ncbi.nlm.nih.gov/23103326/)
29. Cao X, Cui Z, Feng R, Tang YP, Qin Z, Mei B, Tsien JZ. Maintenance of superior learning and memory function in NR2B transgenic mice during ageing. *Eur J Neurosci*. 2007; 25:1815–22.
<https://doi.org/10.1111/j.1460-9568.2007.05431.x>
PMID:[17432968](https://pubmed.ncbi.nlm.nih.gov/17432968/)
30. Bodhinathan K, Kumar A, Foster TC. Intracellular redox state alters NMDA receptor response during aging through Ca²⁺/calmodulin-dependent protein kinase II. *J Neurosci*. 2010; 30:1914–24.
<https://doi.org/10.1523/JNEUROSCI.5485-09.2010>
PMID:[20130200](https://pubmed.ncbi.nlm.nih.gov/20130200/)
31. Haxaire C, Turpin FR, Potier B, Kervern M, Sinet PM, Barbanel G, Mothet JP, Dutar P, Billard JM. Reversal of age-related oxidative stress prevents hippocampal synaptic plasticity deficits by protecting D-serine-dependent NMDA receptor activation. *Aging Cell*. 2012; 11:336–44.
<https://doi.org/10.1111/j.1474-9726.2012.00792.x>
PMID:[22230264](https://pubmed.ncbi.nlm.nih.gov/22230264/)
32. Robillard JM, Gordon GR, Choi HB, Christie BR, MacVicar BA. Glutathione restores the mechanism of synaptic plasticity in aged mice to that of the adult. *PLoS One*. 2011; 6:e20676.
<https://doi.org/10.1371/journal.pone.0020676>
PMID:[21655192](https://pubmed.ncbi.nlm.nih.gov/21655192/)
33. Fossat P, Turpin FR, Sacchi S, Dulong J, Shi T, Rivet JM, Sweedler JV, Pollegioni L, Millan MJ, Olié SH, Mothet JP. Glial D-serine gates NMDA receptors at excitatory synapses in prefrontal cortex. *Cereb Cortex*. 2012; 22:595–606.
<https://doi.org/10.1093/cercor/bhr130>
PMID:[21690263](https://pubmed.ncbi.nlm.nih.gov/21690263/)
34. Junjaud G, Rouaud E, Turpin F, Mothet JP, Billard JM. Age-related effects of the neuromodulator D-serine on neurotransmission and synaptic potentiation in the CA1 hippocampal area of the rat. *J Neurochem*. 2006; 98:1159–66.
<https://doi.org/10.1111/j.1471-4159.2006.03944.x>
PMID:[16790028](https://pubmed.ncbi.nlm.nih.gov/16790028/)
35. Martineau M, Parpura V, Mothet JP. Cell-type specific mechanisms of D-serine uptake and release in the brain. *Front Synaptic Neurosci*. 2014; 6:12.
<https://doi.org/10.3389/fnsyn.2014.00012>
PMID:[24910611](https://pubmed.ncbi.nlm.nih.gov/24910611/)
36. Mothet JP, Rouaud E, Sinet PM, Potier B, Jouvenceau A, Dutar P, Videau C, Epelbaum J, Billard JM. A critical role for the glial-derived neuromodulator D-serine in the age-related deficits of cellular mechanisms of learning and memory. *Aging Cell*. 2006; 5:267–74.
<https://doi.org/10.1111/j.1474-9726.2006.00216.x>
PMID:[16842499](https://pubmed.ncbi.nlm.nih.gov/16842499/)
37. Turpin FR, Potier B, Dulong JR, Sinet PM, Alliot J, Olié SH, Dutar P, Epelbaum J, Mothet JP, Billard JM. Reduced serine racemase expression contributes to age-related deficits in hippocampal cognitive

- function. *Neurobiol Aging*. 2011; 32:1495–504.
<https://doi.org/10.1016/j.neurobiolaging.2009.09.001>
PMID:[19800712](https://pubmed.ncbi.nlm.nih.gov/19800712/)
38. Wolosker H, Dumin E, Balan L, Foltyn VN. D-amino acids in the brain: D-serine in neurotransmission and neurodegeneration. *FEBS J*. 2008; 275:3514–26.
<https://doi.org/10.1111/j.1742-4658.2008.06515.x>
PMID:[18564180](https://pubmed.ncbi.nlm.nih.gov/18564180/)
39. Williams SM, Diaz CM, Macnab LT, Sullivan RK, Pow DV. Immunocytochemical analysis of D-serine distribution in the mammalian brain reveals novel anatomical compartmentalizations in glia and neurons. *Glia*. 2006; 53:401–11.
<https://doi.org/10.1002/glia.20300>
PMID:[16342169](https://pubmed.ncbi.nlm.nih.gov/16342169/)
40. Benneyworth MA, Li Y, Basu AC, Bolshakov VY, Coyle JT. Cell selective conditional null mutations of serine racemase demonstrate a predominate localization in cortical glutamatergic neurons. *Cell Mol Neurobiol*. 2012; 32:613–24.
<https://doi.org/10.1007/s10571-012-9808-4>
PMID:[22362148](https://pubmed.ncbi.nlm.nih.gov/22362148/)
41. Henneberger C, Papouin T, Oliet SH, Rusakov DA. Long-term potentiation depends on release of D-serine from astrocytes. *Nature*. 2010; 463:232–6.
<https://doi.org/10.1038/nature08673>
PMID:[20075918](https://pubmed.ncbi.nlm.nih.gov/20075918/)
42. Yang S, Qiao H, Wen L, Zhou W, Zhang Y. D-serine enhances impaired long-term potentiation in CA1 subfield of hippocampal slices from aged senescence-accelerated mouse prone/8. *Neurosci Lett*. 2005; 379:7–12.
<https://doi.org/10.1016/j.neulet.2004.12.033>
PMID:[15814189](https://pubmed.ncbi.nlm.nih.gov/15814189/)
43. Wolosker H, Blackshaw S, Snyder SH. Serine racemase: a glial enzyme synthesizing D-serine to regulate glutamate-N-methyl-D-aspartate neurotransmission. *Proc Natl Acad Sci U S A*. 1999; 96:13409–14.
<https://doi.org/10.1073/pnas.96.23.13409>
PMID:[10557334](https://pubmed.ncbi.nlm.nih.gov/10557334/)
44. Wolosker H, Panizzutti R, De Miranda J. Neurobiology through the looking-glass: D-serine as a new glial-derived transmitter. *Neurochem Int*. 2002; 41:327–32.
[https://doi.org/10.1016/s0197-0186\(02\)00055-4](https://doi.org/10.1016/s0197-0186(02)00055-4)
PMID:[12176074](https://pubmed.ncbi.nlm.nih.gov/12176074/)
45. Dumin E, Bendikov I, Foltyn VN, Misumi Y, Ikehara Y, Kartvelishvily E, Wolosker H. Modulation of D-serine levels via ubiquitin-dependent proteasomal degradation of serine racemase. *J Biol Chem*. 2006; 281:20291–302.
<https://doi.org/10.1074/jbc.M601971200>
PMID:[16714286](https://pubmed.ncbi.nlm.nih.gov/16714286/)
46. Ploux E, Bouet V, Radzishevsky I, Wolosker H, Freret T, Billard JM. Serine Racemase Deletion Affects the Excitatory/Inhibitory Balance of the Hippocampal CA1 Network. *Int J Mol Sci*. 2020; 21:9447.
<https://doi.org/10.3390/ijms21249447>
PMID:[33322577](https://pubmed.ncbi.nlm.nih.gov/33322577/)
47. Friedman NP, Miyake A. Unity and diversity of executive functions: Individual differences as a window on cognitive structure. *Cortex*. 2017; 86:186–204.
<https://doi.org/10.1016/j.cortex.2016.04.023>
PMID:[27251123](https://pubmed.ncbi.nlm.nih.gov/27251123/)
48. Miller EK, Cohen JD. An integrative theory of prefrontal cortex function. *Annu Rev Neurosci*. 2001; 24:167–202.
<https://doi.org/10.1146/annurev.neuro.24.1.167>
PMID:[11283309](https://pubmed.ncbi.nlm.nih.gov/11283309/)
49. Bizon JL, LaSarge CL, Montgomery KS, McDermott AN, Setlow B, Griffith WH. Spatial reference and working memory across the lifespan of male Fischer 344 rats. *Neurobiol Aging*. 2009; 30:646–55.
<https://doi.org/10.1016/j.neurobiolaging.2007.08.004>
PMID:[17889407](https://pubmed.ncbi.nlm.nih.gov/17889407/)
50. Lacreuse A, Parr L, Chennareddi L, Herndon JG. Age-related decline in cognitive flexibility in female chimpanzees. *Neurobiol Aging*. 2018; 72:83–8.
<https://doi.org/10.1016/j.neurobiolaging.2018.08.018>
PMID:[30237074](https://pubmed.ncbi.nlm.nih.gov/30237074/)
51. Richard's MM, Krzemien D, Valentina V, Vernucci S, Zamora EV, Comesaña A, García Coni A, Intozzi I. Cognitive flexibility in adulthood and advanced age: Evidence of internal and external validity. *Appl Neuropsychol Adult*. 2021; 28:464–78.
<https://doi.org/10.1080/23279095.2019.1652176>
PMID:[31424274](https://pubmed.ncbi.nlm.nih.gov/31424274/)
52. Guidi M, Rani A, Karic S, Severance B, Kumar A, Foster TC. Contribution of N-methyl-D-aspartate receptors to attention and episodic spatial memory during senescence. *Neurobiol Learn Mem*. 2015; 125:36–46.
<https://doi.org/10.1016/j.nlm.2015.07.015>
PMID:[26234588](https://pubmed.ncbi.nlm.nih.gov/26234588/)
53. Neame S, Safory H, Radzishevsky I, Touitou A, Marchesani F, Marchetti M, Kellner S, Berlin S, Foltyn VN, Engelender S, Billard JM, Wolosker H. The NMDA receptor activation by d-serine and glycine is controlled by an astrocytic Phgdh-dependent serine shuttle. *Proc Natl Acad Sci U S A*. 2019; 116:20736–42.
<https://doi.org/10.1073/pnas.1909458116>
PMID:[31548413](https://pubmed.ncbi.nlm.nih.gov/31548413/)
54. Coyle JT, Balu D, Wolosker H. D-Serine, the Shape-Shifting NMDA Receptor Co-agonist. *Neurochem Res*.

- 2020; 45:1344–53.
<https://doi.org/10.1007/s11064-020-03014-1>
PMID:[32189130](https://pubmed.ncbi.nlm.nih.gov/32189130/)
55. Takagi S, Puhl MD, Anderson T, Balu DT, Coyle JT. Serine Racemase Expression by Striatal Neurons. *Cell Mol Neurobiol.* 2022; 42:279–89.
<https://doi.org/10.1007/s10571-020-00880-9>
PMID:[32445040](https://pubmed.ncbi.nlm.nih.gov/32445040/)
56. Wong JM, Folorunso OO, Barragan EV, Berciu C, Harvey TL, Coyle JT, Balu DT, Gray JA. Postsynaptic Serine Racemase Regulates NMDA Receptor Function. *J Neurosci.* 2020; 40:9564–75.
<https://doi.org/10.1523/JNEUROSCI.1525-20.2020>
PMID:[33158959](https://pubmed.ncbi.nlm.nih.gov/33158959/)
57. Balu DT, Takagi S, Puhl MD, Benneyworth MA, Coyle JT. D-serine and serine racemase are localized to neurons in the adult mouse and human forebrain. *Cell Mol Neurobiol.* 2014; 34:419–35.
<https://doi.org/10.1007/s10571-014-0027-z>
PMID:[24436034](https://pubmed.ncbi.nlm.nih.gov/24436034/)
58. Jones EG, Huntley GW, Benson DL. Alpha calcium/calmodulin-dependent protein kinase II selectively expressed in a subpopulation of excitatory neurons in monkey sensory-motor cortex: comparison with GAD-67 expression. *J Neurosci.* 1994; 14:611–29.
<https://doi.org/10.1523/JNEUROSCI.14-02-00611.1994>
PMID:[8301355](https://pubmed.ncbi.nlm.nih.gov/8301355/)
59. McDonald AJ, Muller JF, Mascagni F. GABAergic innervation of alpha type II calcium/calmodulin-dependent protein kinase immunoreactive pyramidal neurons in the rat basolateral amygdala. *J Comp Neurol.* 2002; 446:199–218.
<https://doi.org/10.1002/cne.10204>
PMID:[11932937](https://pubmed.ncbi.nlm.nih.gov/11932937/)
60. Zou DJ, Greer CA, Firestein S. Expression pattern of alpha CaMKII in the mouse main olfactory bulb. *J Comp Neurol.* 2002; 443:226–36.
<https://doi.org/10.1002/cne.10125>
PMID:[11807833](https://pubmed.ncbi.nlm.nih.gov/11807833/)
61. Keaveney MK, Rahsepar B, Tseng HA, Fernandez FR, Mount RA, Ta T, White JA, Berg J, Han X. CaMKII α -Positive Interneurons Identified via a microRNA-Based Viral Gene Targeting Strategy. *J Neurosci.* 2020; 40:9576–88.
<https://doi.org/10.1523/JNEUROSCI.2570-19.2020>
PMID:[33158963](https://pubmed.ncbi.nlm.nih.gov/33158963/)
62. Martina M, Krasteniakov NV, Bergeron R. D-Serine differently modulates NMDA receptor function in rat CA1 hippocampal pyramidal cells and interneurons. *J Physiol.* 2003; 548:411–23.
<https://doi.org/10.1113/jphysiol.2002.037127>
PMID:[12611916](https://pubmed.ncbi.nlm.nih.gov/12611916/)
63. Yang Y, Ge W, Chen Y, Zhang Z, Shen W, Wu C, Poo M, Duan S. Contribution of astrocytes to hippocampal long-term potentiation through release of D-serine. *Proc Natl Acad Sci U S A.* 2003; 100:15194–9.
<https://doi.org/10.1073/pnas.2431073100>
PMID:[14638938](https://pubmed.ncbi.nlm.nih.gov/14638938/)
64. Basu AC, Tsai GE, Ma CL, Ehmsen JT, Mustafa AK, Han L, Jiang ZI, Benneyworth MA, Froimowitz MP, Lange N, Snyder SH, Bergeron R, Coyle JT. Targeted disruption of serine racemase affects glutamatergic neurotransmission and behavior. *Mol Psychiatry.* 2009; 14:719–27.
<https://doi.org/10.1038/mp.2008.130>
PMID:[19065142](https://pubmed.ncbi.nlm.nih.gov/19065142/)
65. Billard JM. Changes in Serine Racemase-Dependent Modulation of NMDA Receptor: Impact on Physiological and Pathological Brain Aging. *Front Mol Biosci.* 2018; 5:106.
<https://doi.org/10.3389/fmolb.2018.00106>
PMID:[30555832](https://pubmed.ncbi.nlm.nih.gov/30555832/)
66. Burke SN, Barnes CA. Neural plasticity in the ageing brain. *Nat Rev Neurosci.* 2006; 7:30–40.
<https://doi.org/10.1038/nrn1809>
PMID:[16371948](https://pubmed.ncbi.nlm.nih.gov/16371948/)
67. Kumar A, Foster TC. Alteration in NMDA Receptor Mediated Glutamatergic Neurotransmission in the Hippocampus During Senescence. *Neurochem Res.* 2019; 44:38–48.
<https://doi.org/10.1007/s11064-018-2634-4>
PMID:[30209673](https://pubmed.ncbi.nlm.nih.gov/30209673/)
68. Samson RD, Barnes CA. Impact of aging brain circuits on cognition. *Eur J Neurosci.* 2013; 37:1903–15.
<https://doi.org/10.1111/ejn.12183>
PMID:[23773059](https://pubmed.ncbi.nlm.nih.gov/23773059/)
69. Koh W, Park M, Chun YE, Lee J, Shim HS, Park MG, Kim S, Sa M, Joo J, Kang H, Oh SJ, Woo J, Chun H, et al. Astrocytes Render Memory Flexible by Releasing D-Serine and Regulating NMDA Receptor Tone in the Hippocampus. *Biol Psychiatry.* 2022; 91:740–52.
<https://doi.org/10.1016/j.biopsych.2021.10.012>
PMID:[34952697](https://pubmed.ncbi.nlm.nih.gov/34952697/)
70. Billard JM, Freret T. Improved NMDA Receptor Activation by the Secreted Amyloid-Protein Precursor- α in Healthy Aging: A Role for D-Serine? *Int J Mol Sci.* 2022; 23:15542.
<https://doi.org/10.3390/ijms232415542>
PMID:[36555191](https://pubmed.ncbi.nlm.nih.gov/36555191/)
71. Avellar M, Scoriels L, Madeira C, Vargas-Lopes C, Marques P, Dantas C, Manhães AC, Leite H, Panizzutti R. The effect of D-serine administration on cognition and mood in older adults. *Oncotarget.* 2016; 7:11881–8.
<https://doi.org/10.18632/oncotarget.7691>

PMID:[26933803](#)

72. Ploux E, Freret T, Billard JM. d-serine in physiological and pathological brain aging. *Biochim Biophys Acta Proteins Proteom*. 2021; 1869:140542. <https://doi.org/10.1016/j.bbapap.2020.140542> PMID:[32950692](#)
73. Birrell JM, Brown VJ. Medial frontal cortex mediates perceptual attentional set shifting in the rat. *J Neurosci*. 2000; 20:4320–4. <https://doi.org/10.1523/JNEUROSCI.20-11-04320.2000> PMID:[10818167](#)
74. Floresco SB, Block AE, Tse MT. Inactivation of the medial prefrontal cortex of the rat impairs strategy set-shifting, but not reversal learning, using a novel, automated procedure. *Behav Brain Res*. 2008; 190:85–96. <https://doi.org/10.1016/j.bbr.2008.02.008> PMID:[18359099](#)
75. Boulougouris V, Dalley JW, Robbins TW. Effects of orbitofrontal, infralimbic and prelimbic cortical lesions on serial spatial reversal learning in the rat. *Behav Brain Res*. 2007; 179:219–28. <https://doi.org/10.1016/j.bbr.2007.02.005> PMID:[17337305](#)
76. Hampshire A, Chaudhry AM, Owen AM, Roberts AC. Dissociable roles for lateral orbitofrontal cortex and lateral prefrontal cortex during preference driven reversal learning. *Neuroimage*. 2012; 59:4102–12. <https://doi.org/10.1016/j.neuroimage.2011.10.072> PMID:[22075266](#)
77. McAlonan K, Brown VJ. Orbital prefrontal cortex mediates reversal learning and not attentional set shifting in the rat. *Behav Brain Res*. 2003; 146:97–103. <https://doi.org/10.1016/j.bbr.2003.09.019> PMID:[14643463](#)
78. Thonnard D, Callaerts-Vegh Z, D'Hooge R. Effects of orbitofrontal cortex and ventral hippocampus disconnection on spatial reversal learning. *Neurosci Lett*. 2021; 750:135711. <https://doi.org/10.1016/j.neulet.2021.135711> PMID:[33571575](#)
79. Young JJ, Shapiro ML. The orbitofrontal cortex and response selection. *Ann N Y Acad Sci*. 2011; 1239:25–32. <https://doi.org/10.1111/j.1749-6632.2011.06279.x> PMID:[22145872](#)
80. Duffy S, Labrie V, Roder JC. D-serine augments NMDA-NR2B receptor-dependent hippocampal long-term depression and spatial reversal learning. *Neuropsychopharmacology*. 2008; 33:1004–18. <https://doi.org/10.1038/sj.npp.1301486> PMID:[17625504](#)
81. Filali M, Lalonde R. The effects of subchronic d-serine on left-right discrimination learning, social interaction, and exploratory activity in APPswe/PS1 mice. *Eur J Pharmacol*. 2013; 701:152–8. <https://doi.org/10.1016/j.ejphar.2012.12.018> PMID:[23276661](#)
82. Labrie V, Lipina T, Roder JC. Mice with reduced NMDA receptor glycine affinity model some of the negative and cognitive symptoms of schizophrenia. *Psychopharmacology (Berl)*. 2008; 200:217–30. <https://doi.org/10.1007/s00213-008-1196-6> PMID:[18597079](#)
83. Nava-Gómez L, Calero-Vargas I, Higinio-Rodríguez F, Vázquez-Prieto B, Olivares-Moreno R, Ortiz-Retana J, Aranda P, Hernández-Chan N, Rojas-Piloni G, Alcauter S, López-Hidalgo M. Aging-Associated Cognitive Decline is Reversed by D-Serine Supplementation. *eNeuro*. 2022; 9:1–15. <https://doi.org/10.1523/ENEURO.0176-22.2022> PMID:[35584913](#)
84. Jett JD, Bulin SE, Hatherall LC, McCartney CM, Morilak DA. Deficits in cognitive flexibility induced by chronic unpredictable stress are associated with impaired glutamate neurotransmission in the rat medial prefrontal cortex. *Neuroscience*. 2017; 346:284–97. <https://doi.org/10.1016/j.neuroscience.2017.01.017> PMID:[28131625](#)
85. Stefani MR, Groth K, Moghaddam B. Glutamate receptors in the rat medial prefrontal cortex regulate set-shifting ability. *Behav Neurosci*. 2003; 117:728–37. <https://doi.org/10.1037/0735-7044.117.4.728> PMID:[12931958](#)
86. Stefani MR, Moghaddam B. Systemic and prefrontal cortical NMDA receptor blockade differentially affect discrimination learning and set-shift ability in rats. *Behav Neurosci*. 2005; 119:420–8. <https://doi.org/10.1037/0735-7044.119.2.420> PMID:[15839788](#)
87. Dalton GL, Ma LM, Phillips AG, Floresco SB. Blockade of NMDA GluN2B receptors selectively impairs behavioral flexibility but not initial discrimination learning. *Psychopharmacology (Berl)*. 2011; 216:525–35. <https://doi.org/10.1007/s00213-011-2246-z> PMID:[21384103](#)
88. Clark E, Antoniuk K, Feniquito A, Dringenberg HC. Effects of the GluN2B-NMDA receptor antagonist Ro 25-6981 on two types of behavioral flexibility in rats. *Behav Brain Res*. 2017; 319:225–33. <https://doi.org/10.1016/j.bbr.2016.11.032> PMID:[27871866](#)
89. Marquardt K, Saha M, Mishina M, Young JW, Brigman JL. Loss of GluN2A-containing NMDA receptors

- impairs extra-dimensional set-shifting. *Genes Brain Behav.* 2014; 13:611–7.
<https://doi.org/10.1111/gbb.12156>
PMID:[25059550](https://pubmed.ncbi.nlm.nih.gov/25059550/)
90. McQuail JA, Beas BS, Kelly KB, Hernandez CM 3rd, Bizon JL, Frazier CJ. Attenuated NMDAR signaling on fast-spiking interneurons in prefrontal cortex contributes to age-related decline of cognitive flexibility. *Neuropharmacology.* 2021; 197:108720.
<https://doi.org/10.1016/j.neuropharm.2021.108720>
PMID:[34273386](https://pubmed.ncbi.nlm.nih.gov/34273386/)
91. Murray TK, Ridley RM, Snape MF, Cross AJ. The effect of dizocilpine (MK-801) on spatial and visual discrimination tasks in the rat. *Behav Pharmacol.* 1995; 6:540–9.
PMID:[11224361](https://pubmed.ncbi.nlm.nih.gov/11224361/)
92. Ward KC, Khattak HZ, Richardson L, Lee JL, Vreugdenhil M. NMDA receptor antagonists distort visual grouping in rats performing a modified two-choice visual discrimination task. *Psychopharmacology (Berl).* 2013; 229:627–37.
<https://doi.org/10.1007/s00213-013-3123-8>
PMID:[23649884](https://pubmed.ncbi.nlm.nih.gov/23649884/)
93. Winters BD, Bartko SJ, Saksida LM, Bussey TJ. Muscimol, AP5, or scopolamine infused into perirhinal cortex impairs two-choice visual discrimination learning in rats. *Neurobiol Learn Mem.* 2010; 93:221–8.
<https://doi.org/10.1016/j.nlm.2009.10.002>
PMID:[19825423](https://pubmed.ncbi.nlm.nih.gov/19825423/)
94. Radke AK, Zweifel LS, Holmes A. NMDA receptor deletion on dopamine neurons disrupts visual discrimination and reversal learning. *Neurosci Lett.* 2019; 699:109–14.
<https://doi.org/10.1016/j.neulet.2019.02.001>
PMID:[30726715](https://pubmed.ncbi.nlm.nih.gov/30726715/)
95. Brigman JL, Daut RA, Saksida L, Bussey TJ, Nakazawa K, Holmes A. Impaired discrimination learning in interneuronal NMDAR-GluN2B mutant mice. *Neuroreport.* 2015; 26:489–94.
<https://doi.org/10.1097/WNR.0000000000000373>
PMID:[25968910](https://pubmed.ncbi.nlm.nih.gov/25968910/)
96. Brigman JL, Rothblat LA. Stimulus specific deficit on visual reversal learning after lesions of medial prefrontal cortex in the mouse. *Behav Brain Res.* 2008; 187:405–10.
<https://doi.org/10.1016/j.bbr.2007.10.004>
PMID:[18022704](https://pubmed.ncbi.nlm.nih.gov/18022704/)
97. Parikh V, Naughton SX, Yegla B, Guzman DM. Impact of partial dopamine depletion on cognitive flexibility in BDNF heterozygous mice. *Psychopharmacology (Berl).* 2016; 233:1361–75.
<https://doi.org/10.1007/s00213-016-4229-6>
PMID:[26861892](https://pubmed.ncbi.nlm.nih.gov/26861892/)
98. Yegla B, Foster TC, Kumar A. Behavior Model for Assessing Decline in Executive Function During Aging and Neurodegenerative Diseases. *Methods Mol Biol.* 2019; 2011:441–9.
https://doi.org/10.1007/978-1-4939-9554-7_26
PMID:[31273715](https://pubmed.ncbi.nlm.nih.gov/31273715/)
99. Yegla B, Boles J, Kumar A, Foster TC. Partial microglial depletion is associated with impaired hippocampal synaptic and cognitive function in young and aged rats. *Glia.* 2021; 69:1494–514.
<https://doi.org/10.1002/glia.23975>
PMID:[33586813](https://pubmed.ncbi.nlm.nih.gov/33586813/)
100. Bean LA, Kumar A, Rani A, Guidi M, Rosario AM, Cruz PE, Golde TE, Foster TC. Re-Opening the Critical Window for Estrogen Therapy. *J Neurosci.* 2015; 35:16077–93.
<https://doi.org/10.1523/JNEUROSCI.1890-15.2015>
PMID:[26658861](https://pubmed.ncbi.nlm.nih.gov/26658861/)
101. Kumar A. Carbachol-induced long-term synaptic depression is enhanced during senescence at hippocampal CA3-CA1 synapses. *J Neurophysiol.* 2010; 104:607–16.
<https://doi.org/10.1152/jn.00278.2010>
PMID:[20505129](https://pubmed.ncbi.nlm.nih.gov/20505129/)
102. Kumar A, Rani A, Tchigranova O, Lee WH, Foster TC. Influence of late-life exposure to environmental enrichment or exercise on hippocampal function and CA1 senescent physiology. *Neurobiol Aging.* 2012; 33:828.e1–17.
<https://doi.org/10.1016/j.neurobiolaging.2011.06.023>
PMID:[21820213](https://pubmed.ncbi.nlm.nih.gov/21820213/)
103. Kumar A, Thinschmidt JS, Foster TC, King MA. Aging effects on the limits and stability of long-term synaptic potentiation and depression in rat hippocampal area CA1. *J Neurophysiol.* 2007; 98:594–601.
<https://doi.org/10.1152/jn.00249.2007>
PMID:[17553951](https://pubmed.ncbi.nlm.nih.gov/17553951/)
104. Barter J, Kumar A, Bean L, Ciesla M, Foster TC. Adulthood systemic inflammation accelerates the trajectory of age-related cognitive decline. *Aging (Albany NY).* 2021; 13:22092–108.
<https://doi.org/10.18632/aging.203588>
PMID:[34587117](https://pubmed.ncbi.nlm.nih.gov/34587117/)
105. Barter J, Kumar A, Rani A, Colon-Perez LM, Febo M, Foster TC. Differential Effect of Repeated Lipopolysaccharide Treatment and Aging on Hippocampal Function and Biomarkers of Hippocampal Senescence. *Mol Neurobiol.* 2020; 57:4045–59.

<https://doi.org/10.1007/s12035-020-02008-y>

PMID:[32651758](https://pubmed.ncbi.nlm.nih.gov/32651758/)

106. Lee WH, Kumar A, Rani A, Foster TC. Role of antioxidant enzymes in redox regulation of N-methyl-D-aspartate receptor function and memory in middle-aged rats. *Neurobiol Aging*. 2014; 35:1459–68.

<https://doi.org/10.1016/j.neurobiolaging.2013.12.002>

PMID:[24388786](https://pubmed.ncbi.nlm.nih.gov/24388786/)

107. Tang LH, Aizenman E. The modulation of N-methyl-D-aspartate receptors by redox and alkylating reagents in rat cortical neurones in vitro. *J Physiol*. 1993; 465:303–23.

<https://doi.org/10.1113/jphysiol.1993.sp019678>

PMID:[7693919](https://pubmed.ncbi.nlm.nih.gov/7693919/)

108. Paxinos G, Watson C. The rat brain in stereotaxic coordinates. 2nd ed. San Diego, CA: Academic Press; 1986.